J. Astrum. Soc. India 25 (3&4) 142-154

A High Spectral Resolution Radiometer for Atmospheric Monitoring

P.C.S. Devara, P.E. Raj, Pandithurai and S. Sharma

Indian Institute of Tropical Meteorlogy, Pune-411008.

Abstract

A high spectral resolution radiometer has been developed and put into operation since April 1993 at the Indian Institute of Tropical Meteorology (IITM) , Pune, India for monitoring of atmospheric aerosols and gaseous constituents. This passive ground-based remote sensor utilizes either sun or moon as light source and measures continuous spectrum of atmospheric extinction from far UV through visible Description of the instrument, experimental and data retrieval techniques, including sample observations, are presented for obtaining atmospheric total, aerosol (Mie), molecular (Rayleigh) and specific gaseous optical depths from spectroradiometer observations carried out on cloud- free days. The derived optical depths are found to be in good agreement with those estimated from in-situ measurements. The temporal and spectral characteristics of aerosol optical depth together with the methods for retrieving the aerosol size distribution and aerosol mass loading from the wavelength distribution of aerosol optical depths are also presented.

1. Introduction

Aerosols and greenhouse gases are of considerable interest in atmospheric sciences. This is mainly due to their potential of changing the radiative transfer of solar radiation, as a direct influence, and due to the complex indirect consequences connected with aerosol-induced cloud and precipitation processes. In recent years, much interest has developed in monitoring of the atmosphere, using remote sensing techniques, especially the possible changes in the earth's radiation budget due to Man's direct influence. While the influence of greenhouse gases on climate can easily be estimated, the consequences arising from an increased (modified) aerosol concentration (due to either human activities or volcanic eruptions) remain extremely difficult to understand because of insufficient knowledge about optical properties of aerosol particles (particularly their vertical distribution), which are strong functions of their sources, sinks and their residence times.

Both active as well as passive ground-based, balloon-borne, air- borne, ship-borne and space-borne experiments, have been conducted for studying the properties of aerosols and gas molecules and their interaction with radiation passing through the atmosphere. Of these, sun photometry, being a simple passive technique, has been widely used by Angstrom (1961) for extensive long-term studies of aerosols and some selected trace gas species. A long series of atmospheric turbidity (attenuation) measurements have also been carried out at different stations in India by using Volz sun-photometers (Mani et al., 1969). Subsequently , this instrument has undergone many modifications in both spectral coverage and then data acquisition (Shaw et al.,

1973, Pitts et al., 1977, Asano et al., 1993). Recently, a Multi- Wavelength Solar Radiometer (MWR) experiment (as a pat of the IMAP) has been performed at six stations covering different geographical locations in India (Krishna Moorthy et al., 1989). The results of these observations collected at nine narrow spectral bands (5nm FWHM) in the visible and near IR regions for a period of about 5 years have revealed significant temporal and spectral variation in bulk characteristics of aerosols present in different environments in India. However, all these studies have been performed at discrete wavelengths (or spectral bands) and the total observations time was high as compared to the short-term changes in aerosol characteristics due to environmental and local meteorological factors such as wind. Moreover, broader wavelength range with narrow spectral interval is an important requirement in deriving better information on physico-chemical characteristics of aerosol particles which are present in the atmosphere in different sizes (from $10^{-3}\mu m$ to $10^{3}\mu m$) with varying chemical composition. The High Spectral Resolution Radiometer, described in this paper, has been developed to meet most of these requirements such as continuous scanning of solar spectrum in a specified wavelength region at a faster rate so that the information content will give better estimation of atmosphere aerosol and trace gas constituents. We shall describe the experimental set-up and data retrieval technique and discuss the result of atmospheric total as well as aerosol optical depth variations as computed from High Spectral Resolution Radiometric observations and *in-situ* measurements in the following sections.

2. Theoretical background

The basic principle involved in radiometers aimed at determining atmospheric optical depth is that extraterrestrial solar (or lunar) radiation undergoes modification when passing through the atmosphere resulting in and a general decrease of the spectral irradiance with increasing air mass (i.e. The length of the atmospheric path traversed by the sun' or moon's rays in reaching the earth measured in terms of the length of this path when the sun or moon is in the zenith). This decrease is mainly due to extinction (scattering plus absorption) of light by aerosols and gas molecules. Thus the measurement of relative flux of either sun or moon radiations at the earth's surface as function of zenith angle provides optical depth or optical thickness and related basic quantities such as extinction or attenuation or turbidity or visibility etc.

As explained by many investigators (Yamamoto and Tanaka, 1969, quenzel, 1970, Herman et al., 1971, Shaw et al., 1973., King et al., 1980) the signal output of radiometer represents monochromatic solar irradiance, F ($\lambda\chi$) reaching the ground at wavelength λ, and related to the irradiance incident on the top of the atmosphere, Fo(λ) through the well known Beer-Bouguer-Lambert law as

$$F(\lambda,\chi) = (Z_m/Z)^2 \, Fo(\lambda) \exp[-m(\chi)\,\tau_t(\lambda)] + F_d(\lambda,\chi) \qquad (1)$$

where Z_m is mean distance between the earth and light source, Z is distance between the earth and light source at the time of observation, m is optical air mass which is a function of zenith angle, ($m=\text{Sec}\,\chi$ for $\chi < 800^{o}$), F_d (λ,χ) diffusely scattered flux at wavelength λ entering the radiometer, generally, contribution of F_d to the total observed direct radiation is meagre for radiometers having narrow field of view, and hence can be neglected (herman et al., 1971)

The total optical depth, $\tau_t(\lambda)$, of a vertical air column at wavelength λ is represented mathematically by sum of three components as

$$\tau_t(\lambda) = \tau_R(\lambda)\, P/P_o + \tau_a(\lambda) + \tau_g(\lambda) \qquad (2)$$

where $\tau_t(\lambda)$ is optical depth due to Rayleigh scattering by air molecules, P and po are atmospheric pressures at the place of observations and at sea level for a standard atmosphere, respectively, $\tau_g(\lambda)$ is optical depth arising from absorption by atmospheric gases such as nitrogen dioxide, ozone, water vapour, oxygen and carbon dioxide etc. and $\tau_a(\lambda)$ is optical depth resulting from extinction by aerosols $\tau_R(\lambda)$ can be computed from the Rayleigh scattering cross-section and the molecular number density of the atmosphere. Similarly $\tau_a(\lambda)$ can be evaluated from the absorption coefficients and height profiles of relevant gases can be obtained by subtracting $\tau_R(\lambda)$ and $\tau_g(\lambda)$ from $\tau_t(\lambda)$ as shown in Eq. (2).

It is customary to represent Eg. (1) in logarithmic form, neglecting F_d, as

$$\text{In } F(\lambda,\chi) = 2 \text{ In } (Z_m/Z) + \text{ In } F_o(\lambda) - m(\chi)\, \tau_t(\lambda) \qquad (3)$$

The radiometer output signal, being linearly related to $F(\lambda,\chi)$ in the above equation, a plot between in $F(\lambda,\chi)$ and $m(\chi)$ will yield a linear curve (known as Langley plot), the slope of which gives $\tau_t(\chi)$. As seen from Eq. (2), optical depths (or column content) of atmospheric gases also can be retrieved from radiometric observations collected at different wavelengths corresponding to absorption bands of gaseous molecules (Shaw, 1979). The signal corresponding to zero air mass at each wavelength provides absolute calibration of the radiometer and it can be determined by extrapolating the straight line fitted to the data points and noting its intercept on the Y-axis

3. Description of spectroradiometer

The High Spectral Resolution Radiometer (hereafter called as HSRR) used to measure atmospheric optical depth composed of mainly three parts: (i) an automatic tracking system to follow the motion of either sun or moon; a double monochromator for spectral analysis of measured irradiance and (iii) an on-line data acquisition, analysis and plotting system. An optical electrical line drawing of the HSRR is shown in Fig. 1. The radiations either from sun or moon are brought continuously inside the laboratory (through a wall-cutout) to the rest of the experimental set-up by means of a tracking system which was mounted equatorially and driven by a synchronous motor. This tracking system was installed on the terrace of the institute building in order to make the system free from nearby tall topographic objects and also from city light pollution during nighttime so that observations from either sun or moon can be recorded almost at all zenith angles. The system was calibrated with the pole star and set to geographical location of the experimental site so that it can follow the light source automatically without much manual intervention and the tracking accuracy was about 0.5°/day. However, the system requires adjustment occasionally for better alignment between the input radiation and entrance slit of monochromator due to initial settings based on temporal variations in rise and/or set timings of the light source. Moreover, these adjustments will not affect the measurements as the time required for each set of observations collected over a wide wavelength range at faster scan rate for the present study (λ200-720 nm scanned at a rate of 5 nm/sec) is very small i.e. 1 minute 45 seconds. The radiations were passed through baffles and a shutter, which prevent entrance of stray light into the monochromator and provides observations of detector's dark current noise, respectively. The later observations corresponding to no input radiations (shutter close period) provide a check for the stability of the electronic circuitry.

The Spex Model 1680 B double monochromator used for the spectral analysis of input radiations at high resolution consists of holographic diffraction gratings (1800 grooves/mm) and was operated in the spectral range between 200 and 720 mm with an accuracy (Full Width at Half

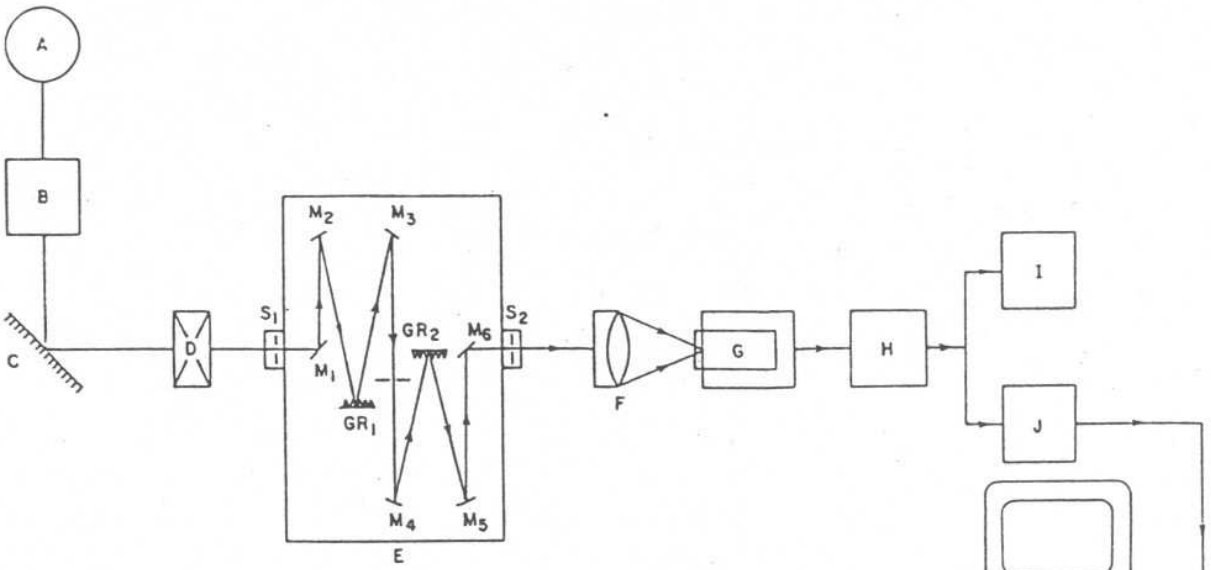

A : SOURCE (SUN OR MOON)
B : HELIOSTAT OR SUN(MOON) TRACKER
C : REFLECTING MIRROR
D : SHUTTER
E : DOUBLE MONOCHROMATOR
S_1: ENTRANCE SLIT
S_2: EXIT SLIT
M_1, M_2, M_4, M_6: REFLECTING MIRRORS
M_3 & M_5 : COLLIMATING MIRRORS
GR_1 & GR_2 : HOLOGRAPHIC GRATINGS
F : CONDENSING LENS
G : PHOTOMULTIPLIER WITH COOLER HOUSING
H : AMPLIFIER (ANALOG OR PHOTON COUNTING)
I : MULTIPEN CHART RECORDER
J : INTERFACE
K : DATA ACQUISITION, ANALYSING & PLOTTING SYSTEM

Fig. 1. Schematic of high spectral resolution radiometer

Maximum) of ± 0.4nm. The spectral sampling interval as well as the number of spectra for averaging can be set according to experimental requirements. For the present measurements, a sampling interval of 5 mm for each spectrum was used. The project field of view of the instrument was ~ 1° × 4°. As this field of view is larger than the apparent field of view of either solar or lunar disk (~0.5°), some portion of diffuse sky irradiance enters into the HSRR. However, the estimated diffuse light contamination is very small (not more than 0. 5%) as compared to the measured irradiance and hence can be neglected (Reagan et al., 1986)

The received radiations, after spectrally analysed and condensed, were focused on to an EMI Model 9659QB,S-20 cathode photomultiplier (PMT). The PMT has spectral response from 200 to 900 nm with quantum efficiency up to 20% and gain of 0.6×10^6 the PMT was cooled to about –20°C by means of a PFR Model TE-206 TSRF cooler housing to reduce the level of dark current noise to minimum when the moon was used as light source. The output of the PMT was discriminated to increase the signal-to-noise ratio and further amplified by a low-noise, variable gain amplifier. The amplified analog signal was digitized to 12 bits using IC AD7880. The signals were recorded simultaneously on a high-speed chart recorder for visual inspection of the

characteristics of each spectrum of irradiance and were also acquired by a mini-computer after multiplexing with the time information provided by a master clock for on-line storing of the spectra on floppy diskette, their real-time analysis and plotting. The main specifications of the HSRR are given in Table 1.

Table 1 Day-to-day variations in ln $F_o(\lambda)$ with wavelength

F(λ) Date	400 nm	550 nm	700 nm	1060 nm	1630 nm
01.11.1993	2.275	3.094	2.604	4.605	3.748
02.11.1993	2.174	2.917	2.499	4.574	3.826
03.11.1993	1.934	2.975	2.473	4.611	3.6691
04.11.1993	2.081	2.955	2.429	4.460	3.825
05.11.1993	1.610	3.097	2.628	4.480	3.772
AVG ln F(λ)	2.015	3.088	2.527	4.546	3.772
Standard Error (%)	4.6	1.48	1.53	2.9	2.3

4. Acquisition and analysis of observations

The atmospheric optical thickness, presented in this paper, were derived from the spectral attenuation measurements of direct solar irradiance made with the HSRR during April-June and October-December 1993 from the terrace of the Institute's building 12.5 m above the ground. The terrain characteristics of the experimental site as well as meteorological and environmental conditions of the observing station can be found in a recent publication by authors (Devara et al., 1994). The observations were made from morning till evening on the days when the sky was nearly free of visible clouds, and none were near the line-of- sight to the sun. The observations were repeated at an interval of 5 minutes during the periods of sunrise and sunset when the variation of zenith angle with time is faster, at 30-minute interval during the intervening period. Sometimes these measurement intervals were considered to be nominal intervals for essentially unchanging sky conditions. In each set of observations, noise was recorded for few seconds (by closing the shutter) prior to the measurement of irradiance spectrum over the wavelength range of interest. The average value of noise was subtracted from the values of irradiance recorded for different wavelengths at each time of observations. Thus the spectra containing the signal values of solar irradiance recorded over a wavelength range at different times of the day, after normalizing with the monochromator grating response, were subjected to further analysis of deriving temporal and spectral variability of atmospheric optical depth.

An Volz sun-photometer (hereafter called as SP) whose details have been published by Mehra et al (1986) was also operated in conjunction with the HSRR for comparison. This photometer has a selenium barrier photocell to detect quasi-monochromatic solar irradiance at five wavelengths,

which were chosen by narrowband (FWHM of 2nm) interference filters with peak transmissions at 400, 600, 940, 1060 and 1630 nm. Four wavelengths were used for aerosol observations with the exception of 940 nm which coincided with absorption band of water vapour. It may be noted that the fact here to use two different instruments operating on similar principle is a very good mean to determine and intercompare the atmospheric optical depths. The result of such comparison also provide a check for the contamination of signals at larger wavelength due to higher orders of grating diffraction effects. The close agreement between the optical depths estimated by the HSRR and SP reveals that the effect of higher order diffraction models in the wavelength range of interest in negligible.

Zenith angles (χ) and corresponding air mass m (χ) values for each observations were computed with the aid of solar declination angle (δ) and hour angle (H) obtained for the day from the Indian Astronomical Ephemeris (1993) using the following expression

$$\cos\chi = \sin\delta + \cos\delta \cos\phi \cos H \tag{4}$$

where ϕ is latitude of observing station i.e.18° 32'N. This expression can be used for obtaining air mass values (approximately equivalent to sec χ) only up to zenith angles <80. The empirical expression for air mass suggested by Rozenberg (1966), i e.,

$$m(\chi) = (\cos\chi + 0.025\, e^{-11\cos\chi})^{-1} \quad -11\cos\chi)^{-1} \tag{5}$$

was used to calculate air mass for Zenith angles, $\chi > 80$. The second term in this expression accounts for the curvature of the earth- atmosphere system and atmospheric refraction.

The following expression suggested by Teillet (1990) was used to estimated the Rayleigh optical depth, τ_R in Eq. (2)

$$\tau_R(\chi) = [(8\pi^2(n^2-1)^2 N_c)/(3\lambda^4 N_s^2)]\,(6+2\gamma)/(6-7\gamma)](P/P_o)(T_o/T) \tag{6}$$

where n is refractive index of air molecules; N_c is columnar number density of air at any atmospheric pressure and temperature; N_s is molecular number density at S.T.P.; γ is the depolarization ratio for transverse scattering of depolarized light; P and T are station surface pressure and temperature; P_o and T_o are pressure and temperature for standard conditions, respectively. King's correction values for Rayleigh depolarization factor in Eq. (6) i.e [(6+3γ)/ (6-7γ)] for different wavelengths obtained from Bates (1984) have been used in the present study.

The refractive index of air molecules, n was evaluated at different wavelengths, using the expression suggested by Kneizys et al (1980), i.e.,

$$10^6(n-1) = (77.46 + 0.459\lambda^2)\,(1013,25/288.15 \tag{7}$$

The reference atmosphere for Indian equatorial zone from surface to 80 Km by Sasi and Sen Gupta (1985) has been used in the evaluation of N_c in Eg. (6) and the upper limit for integration was considered up to 50 km for the present study as this accounts for almost the total neutral atmosphere.

Although nitrogen dioxide and oxygen have weak absorption at all wavelengths considered in the present study, water vapour and ozone have significant absorption near 700 nm and in the Chappuis band (400-650 nm), respectively, and hence they cannot be neglected. Extinction due to O_3 absorption (known as ozone optical depth), $\tau_g(\lambda)$ in Eq. (2) was computed by using the relation

$$\tau_{o3}(\lambda) = \sigma_{o3}(\lambda) \int N_{o3}(h)\, dh \tag{8}$$

Where σ_{o3} and N_{o3} are absorption coefficient and number density of ozone over an altitude range dh centered about h. The ozone absorption coefficients at different wavelengths in the Chappuis band as given by Kneizys et al. (1980) and the ozone number density model profile for Pune constructed by matching the balloonsonde observations reported by Kundu (1982) and the rocket observations reported by Acharya et al. (1984) have been used in the estimation of $\tau_{o3}(\lambda)$ Extinction due H_2O absorption at 700 nm was computed by following the method described by Krishna Moorthy et al. (1988). Thus once the values of $\tau_t(\lambda)$, $\tau_R(\lambda)$ are known, $\tau_a(\lambda)$ can be reckoned from Eq.(2).

5. Discussion of Results

Some of the results obtained from the experiments conducted on cloud-free days during April-June and October-December 1993 are presented and discussed in the following sections.

5.1 Determination of total optical depth and system constant

The radiometric methods of determining atmospheric optical depth involves mainly two assumptions. One is that radiometer output and incident solar flux are linearly related and the other is that extinction properties of atmosphere remain constant during the observations. Moreover, the instrument does not require a priori knowledge of the absolute calibration constants because the linear regression fitted line passing through the date points is used to calculate the optical depth. However, as explained by Stair and Ellis (1968), absolute calibration of the instrument can be obtained by referencing the extrapolated zero airmass signal to the known values of incident solar radiation.

Figure 2 illustrates a typical Langley plot of observations recorded on 3 November 1993 at ten wavelengths ranging from 400 to 1630nm. The data for seven wavelengths between 400 and 700 nm at 50 nm interval were obtained from the HSRR and data for five wavelengths (400, 600, 940, 1060 and 1630 nm) were obtained with the SP simultaneously. Inspection of the figure reveals linear variation of date points in accordance with Eq. (3) . In each plot, the total optical depth (TAU) value together with its standard error (SE) at wavelength of observations are also shown. These values in the case of SP are shown in the figure as TAUP and SEP, respectively. It can be seen that the total optical depth, on an average, varies significantly with wavelength and the associated standard errors are insignificant (<2%). Moreover, a close agreement can be seen between the optical depths estimated from the observations of HSRR and SP at their common wavelengths (400 and 600 nm). Any deviation between such measurements can be attributed to differences in the fields of view of HSRR and SP; and to the finite bandwidth of filters used in the SP. In addition to the slope, the values of ln $F_o(\lambda)$ corresponding to zero air mass, other statistical parameters like correlation coefficients and variance of $\tau_t(\lambda)$ were also computed for each set of observation and are used to clean the data sets by removing spurious points that arise either due to misalignment of optics or due to short-term variations of the atmosphere (or due to instrumental or atmospheric drift)

The Y-axis intercept in Fig. 1 yield [in (F_o) + 2in (Z_m/z)], from which in $[F_o(\lambda))]$ was computed for all the days of observations. These zero air mass intercepts obtained for different wavelengths from day to day should remain constant for clear stable days and any variations in it over a period of time reveal changes (drift) in the system characteristics. The determination of $\tau_t(\lambda)$ is sensitive even to small errors in the measurement of ln $[F_o(\lambda)]$, and it is difficult to determine ln $F_o(\lambda)$ from observations on a single day because of the stringent requirements on the optical stability of the

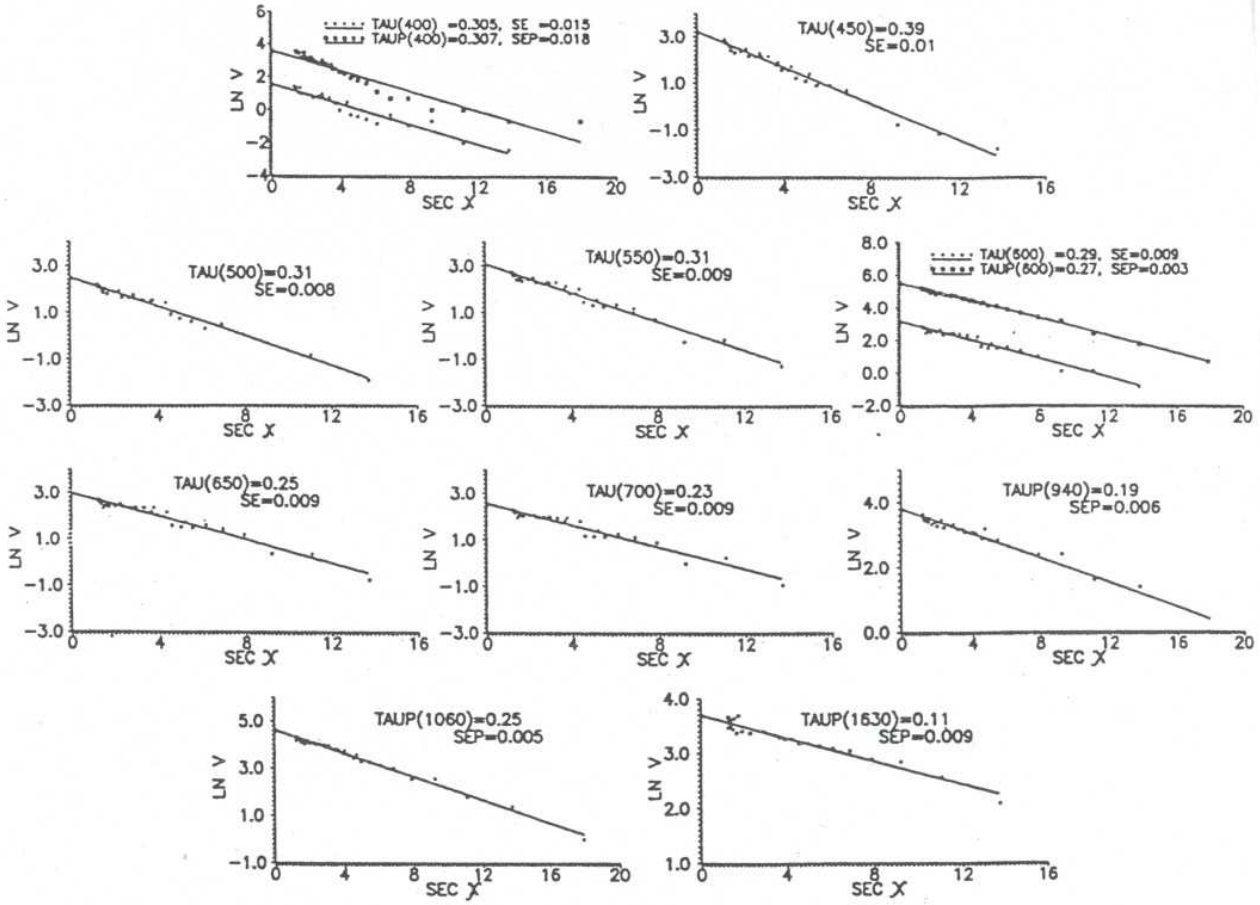

Fig. 2. Langley plot for different wavelengths obtained on 03 Nov. 93

atmosphere Therefore, it is essential to calibrate the radiometer based on average ln $[F_o(\lambda)]$ determined from all the stable-day Langley plots over a period of time. Such calibration procedures using weighted average intercepts have been suggested by Young (1962) . In order to examine day to day variations in calibration constant, the values of in $[F_o(\lambda)]$ for all wavelengths used in the present study were calculated as explained above. As an example, such values obtained for specific wavelengths of 400, 550. 700, 1060 and 1630 nm on five successive days in November 1993 are presented in Table 2. This table also presents the average ln $[F_o(\lambda)]$ along with the standard errors. It can be noted that the standard error values are very small indicating that the changes in system characteristics are insignificant.

Table 2 Variation of junge exponent (v) on different days of observation

Date	v	Std. Error (%)
23.04.1993	2.47	1.0
28.04.1993	2.27	3.7
05.05.1993	2.44	3.3
19.05.1993	2.61	4.3
01.11.1993	2.57	4.0
03.11.1993	2.85	2.6

5.2 *Spectral distribution of atmospheric optical depth*

Once the total optical depth [$\tau_t(\lambda)$]has been determined, one can determine the corresponding values of aerosol optical depth [$\tau_a(\lambda)$]from Eq. (2) by subtracting from $\tau_t(\lambda)$, the contributions due to molecular scattering $\tau_R(\lambda)$, known as the Rayleigh optical depth, and the contributions of ozone Chappuis absorption band and water vapour, $\tau_g(\lambda)$. Further correction to the total optical depth may be necessary if the wavelengths have been selected in bands of strong selective absorption by other atmospheric gases. Figure 3 shows typical spectra of total optical depth and aerosol optical depth following of Rayleigh and molecular optical depth obtained from the observations of HSRR on 3 November 1993. The optical depths derived from concurrent observations collected with SP at discrete wavelengths are also plotted in the figure. The high spectral resolution observations of HSRR reveals variations in optical depths at narrow spectral bands in the entire wavelength range in question and such variations are missing in the SP which was operated at discrete wavelengths. By considering the close agreement observed between optical depths deduced from HSRR derived and SP (as shown in Figs. 2 and 3), the HSRR optical depths are joined (by broken line) with those derived from SP at near IR wavelengths of 1060 and 1630 nm, so as to examine the spectra dependence of total as well as aerosol optical depths over a wide wavelength range. Multiwavelength measurements of aerosol optical depths of the type presented in Fig. 4 can be used to infer the size distributions of atmospheric aerosols. Numerous size distributions have been reported from in-situ and remote sensing observations, and several analytical expressions have been

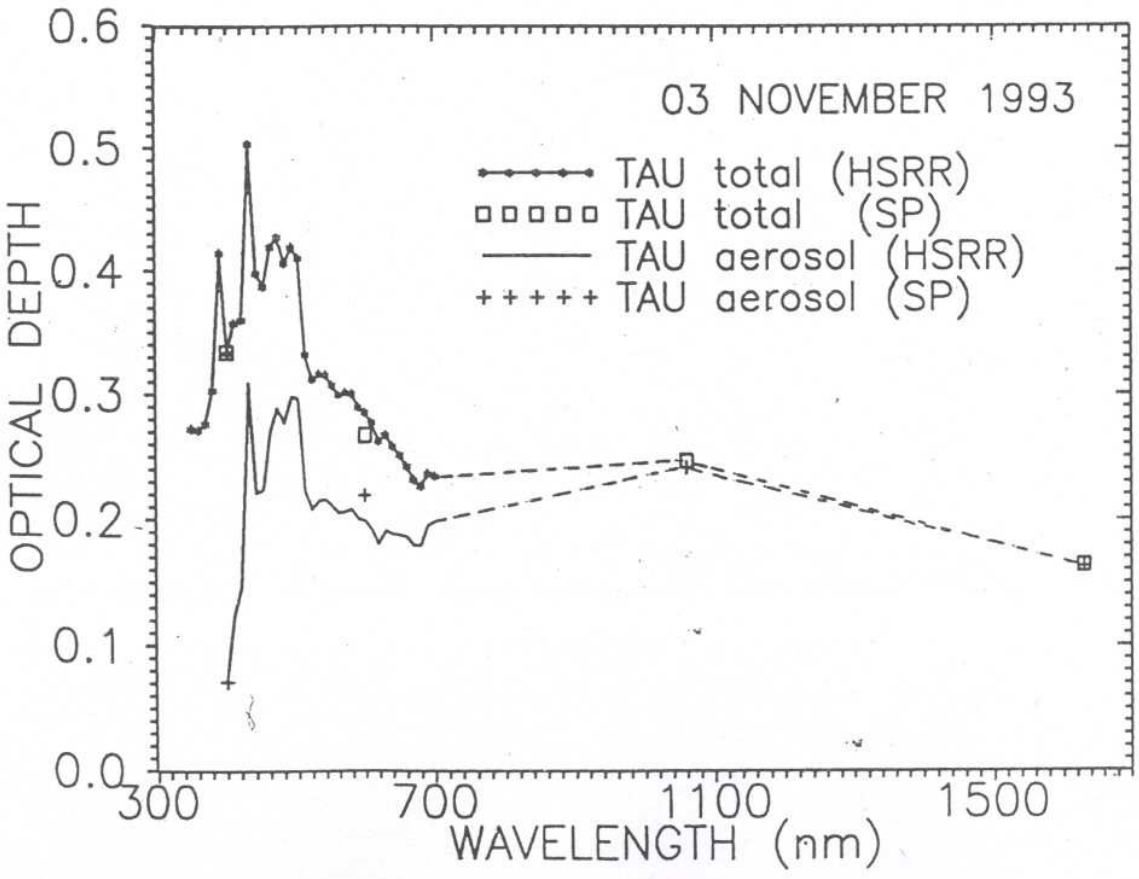

Fig. 3. Wavelength distribution of optical depths observed on 03 Nov. 93

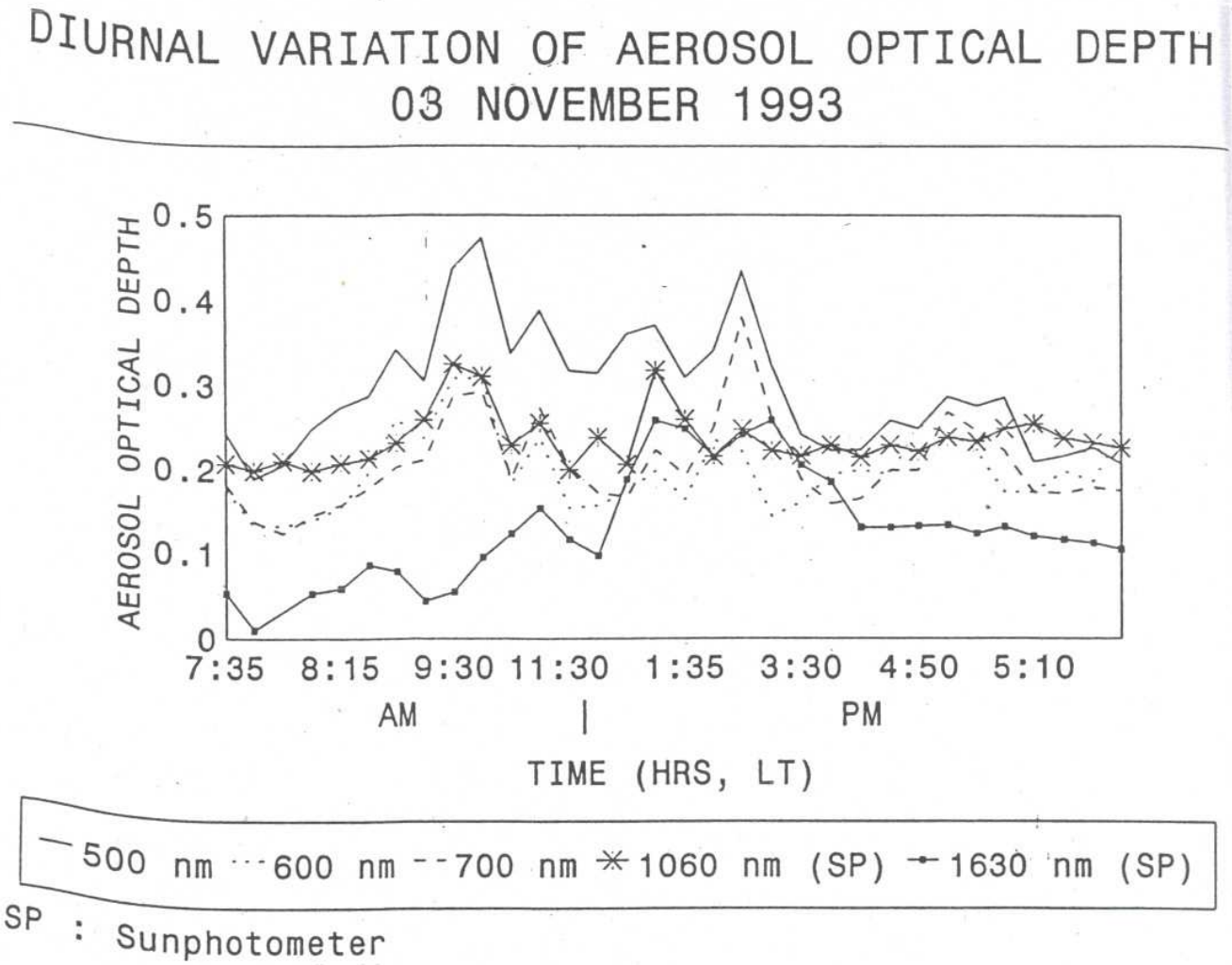

Fig. 4. Temporal spectral variation of aerosol optical depths observed on 03

proposed. Such an attempt has also been made in this paper. In order to simplify the data analysis and avoid having more free parameters than can be reliably fitted by the observations, a simple power-law size distribution, first proposed by Junge (1963), of the following type has been used in the present study.

$$n(r) = dN/dr = C_r - (v+1) \quad (8)$$

where N is number of aerosol particles per unit volume up to radial size r and C is a scaling constant. The parameter v is often called as the junge parameter or junge exponent or shaping constant, which generally lies between 2 and 4. McCartney (1976) showed that, if the aerosols follow a power-law size distribution, the relationship between aerosol optical depth and wavelength also follows a power-law as

$$\tau_a(\lambda) = \text{Const.}\, \alpha^{-\alpha} \text{ with } v = \alpha + 2 \quad (9)$$

Therefore, the slope of the linear regression fit between log $[\tau_a(\lambda)]$ and log (λ) yields the value of α and hence v. The values of v, together with standard error, retrieved from the wavelength dependence of aerosol optical depth plots obtained from the HSRR observations recorded on two selected days each in the month of April, May and November 1993 are presented in Table 2.The retrieved values of v were found to be statistically significant (>95%) with error varying between 3

and 14% and they are consistent with the columnar size distributions of urban atmospheric aerosols reported in the literature (King et al., 1978). By evaluating the scaling constant using the radial range i.e.lower and upper limits for aerosol size distributions can be studied from Eq. (8)

5.3 *Time variation of aerosol optical depth*

Using the average in $[F_o(\lambda)]$ values and the data of incident solar flux recorded at different times of the day, $\tau_a(\lambda)$ values were re-evaluated for different wavelengths. Such temporal variations observed on a typical day (3 November 1993) are shown plotted in Fig. 4. The time evolution of optical depth at all the wavelengths, as seen from the figure, shows significant variations during the course of the day with lower depths during morning and evening hours and higher depths during afternoon hours. The variations in the aerosol optical depths during mid- day hours could be explained on the basis of advection of pollution from surroundings and convective activity leading to changes in aerosol particle number distributions and gas-to- particle conversions (photochemical processes) while those during forenoon hours could be attributed to the impact of radiative cooling and turbulent processes on aerosol characteristics during previous night. Short-term variations in optical depth and their relationship with meteorological parameters can also be studied by properly grouping the observations as forenoon and afternoon with respect to the local noon (time of minimum of χ).

5.4 *Computation of aerosol mass loading*

Having determined the values of v, columnar aerosol mass load computation of aerosol loading station can be estimated by following the method suggested by shaw et al. (1973) using the expression

$$m_L = K[\tau_a(\lambda_{500}) / \beta_{500})] \quad (10)$$

where K is numerical value os mass loading (typical value of 200 $\mu g/m^3$ representative of urban station) used for calculation of aerosol extinction coefficient, $\tau_a(\lambda_{500})$ an $\beta_{500})$ are aerosol optical depth and extinction coefficient at wavelength of 500 nm, respectively. Such computations have also been attempted in this paper using aerosol optical depths evaluated from HSRR observations collected on 28 April and 3 November 1993. The columnar aerosol loading over the experimental station were 1.373 and 0.4098 $\mu gm/m^2$ on 28 April and 3 November 1993, respectively, which are consistent with the values reported in the literature (Shaw et al., 1973)

Acknowledgements

The authors would like to express their gratefulness of Professor. R.N. Keshavamurty, Director IITM, Pune and Dr. A.S.R. Murty for their support and encouragement.

References

Acharya, Y.B., Jayaraman, A. and Subbaraya, B.H., 'The ozonesonde intercomparison experiment at Thumba', *Proc.XXV COSPAR*, Grez (1984)

Angstrom, A., 'Techniques of determining the turbidity of the atmosphere', *Tellus*, **13**, 213-223 (1961)

Asano, S., Uchiyama, A. and Shiobara, M., 'Spectral optical thickness and size distribution of Pinatubo volcanic aerosols as estimated by ground-based photometry', *J. Meteor. Soc. Japan*, **71**, 165-173 (1993).

Bates, D.R., 'Rayleigh scattering by air', *Planet Space Sci.*, **32**, 785-790 (1984)

Devara, P.C.S., Raj, P.E, .Sharma, S and Pandithurai, G.'Lidar- observed long-term variations in urban aerosol characteristics and their connection with meteorological parameters', *Int, J. Climatol.*, **14**, 581-591 (1994)

Herman, B.M., Browning, S.R and Curran, R.J., 'Effect of atmospheric aerosols on scattered sun light', *J, Atmos. Sci.*, **28**, 419-428 (1971).

Indian Astronomical Ephemeris, IMD, Calcutta, (1993)

Junge, C.E., 'Air Chemistry and Radioactivity', Academic Press, New York (1963).

King, M.D., Byrne, D.M., Herman, B, M.and Began, J.A., 'Aerosol size distributions obtained by inversion of spectral optical depth measurements', *J. Atmos. Sci.*, **35**, 2153-2167 (1978).

King. M.D., Byrne, D.M., Reagan, J.A.and Herman, B.M., 'Spectral variation of optical depth at Tucson, arizona between August 1975 and December 1977', *J. Appl. Meteorol.*, **19**, 723-732, (1980).

Kneizys, F.X, Shettle, E.P., Gallery, W.O., Chetwynd, J.H., Abreu, L.W., Selby, J.E.A., FennR.W and McClatchey, R.A., Atmospheric Transmittance/Radiance Computer code LOWTRAN 5', AFGRL-TR-80-0067, AFGL, Massachusets, USA, (1980)

Krishna Moorthy, K., Nair, P.B. and Krishna Murty, B.V, 'A study on aerosol optical depth at a coastal station, Trivandrum', Indian J. Radio &Space phys., 17, 16-22 (1980).

Krishna Moorthy, K., Nair, P.B and Krishna Murty, B.V., 'Multiwavelength solar radiometer network and features of aerosol spectral optical depth at Trivandrum', *Indian J. Radio & Space Phys.*, **18**, 194-201 (1989)

Kundu, N., N'Reference ozonosphere over India', ISRO-IMAP-SP-09- 82, ISRO, Bangalore, India, (1982)

Mani, A., Chacko, O and Hariharan, S., "A study of Angstrom turbidity parameters from solar radiation measurements in India', *Tellus*, **21**, 829-843 (1969)

McCartney, E.J., 'Optics of the Atmosphere:Scattering by Molecules and Particles', Wiley, New York (1976)

Mehra, P.M., Vijayakumar, R. and Mary Selvam, A., 'Measurement of atmospheric total ozone by the filter photometric technique', *J Atmos Chem.*, **4**, 335-342 (1986)

Pitts, D.E., AcAllum, W.E., Heidt, M and Jeske, K., 'Temproal variations in atmospheric wate vapor and aerosol optical depth determined by remote sensing', *J Appl. Meteor.*, **16**, 1312-1321 (1977)

Quenzel, H., 'Determination of size distribution of atmospheric aerosol particles from spectral solar radiation measurements', *J. Geophys, Res.*, **75**, 2915-2921 (1970)

Reagan, J.A., Thomson, L.W., Herman, B.M. and Palmer, J.M., 'Assesment of atmospheric limitations on the determination of the solar spectral constant from ground-based spectroradiometer measurements', IEEE Trans.Geosci. Remote sensing GRS-**24**, 258-266 (1986)

Rozenberg, G.V., 'Twilight:A study in Atmospheric Optics' (English translation), Plenum Press, (1966)

Sasi, M.N. and Sen Gupta, K., 'A reference atmosphere for Indian equatorial zone from surface to 80km', Sci. Rep., SPL:SR:006:85, SPL, VSSC, Trivandrum, (1986).

Shaw, G.E., 'Aerosols at Mauna Loa:Optical properties', *J, Atmos. Sci.*, **36**, 862-869 (1979).

Shaw, G.E., Regan, J.A. and Herman, B.M., 'Investigations of atmospheric extinction using direct solar radiation measurements made with a multiple wavelength radiometer', *J. Appl Meteorol.*, **12**, 374-380 (1973)

Stair, R. and Ellis, H.T., 'The solar constant based on new spectral irradiance data from 310 to 530 nanometers', *J. Appl. Meteorol.*, **7**, 635-644 (1968)

Teillet, P.M., 'Rayleigh optical depth comparisons from various sources', *Appl.Opt.*, **29**, 1897-1900 (1900)

Volz, F.E., 'The optics and meteorology of atmospheric turbidity', Ber. Deutch. Wetterd, 2, (1954).

Yamamoto, G. and Tanaka, M., Determination of aerosol size distributions from spectral attenuation measurements', *Appl. Opt.*, **8,** 447-453 (1969).

Young, T., 'Revised depolarization corrections for atmospheric extinction', *Appl. Opt.*, **19**, 3427-3428 (1980)